



Smart Grid Operation with Hybrid Renewable Resources and Electric Vehicle

Mohamed Ahmed Hassan El-Sayed

Electrical Engineering Department, College of Engineering & Petroleum, Kuwait University
(On leave from Cairo University)

Phone:+0096566033591, e-mail: elsmah@hotmail.com

Abstract. The utilization of renewable energy resources will significantly increase to achieve clean and sustainable electricity generation. The management of the continuous growth share of variable renewable resources, integration of electric vehicles (EVs) and regulation of grid frequency require effective communication facilities of recent smart grids. In this respect, smart converters can provide efficient power conditioning devices to extract maximum power from renewable resources. In addition, the batteries of EVs could be used as distributed storage and discharge power back into the grid to compensate power deficit and fluctuation.

Modeling and controlling of the hybrid resources within smart grid were carried out in this paper. The smart converter is switched to track the maximum power point MPPT of the solar panels. In addition, the pitch angle control and DFIG regulation are used to extract the maximum power under different wind speed and tidal stream velocities. The deployment of EVs can compensate power fluctuations and regulate the frequency deviations in the grid based on the proposed PID controller. In this paper, the integral minimization of time-weighted absolute error (ITAE) is used for on-line tuning of the PID controller parameters. Using Matlab/Simulink package, the smart grid is modeled and simulated using the weather data of Kuwait and then the grid performance is assessed under system disturbances and load excursions.

Key words

Solar, Wind, Tidal Energy, Electric Vehicle, Smart Grid.

1. Introduction

Recently, there is an increasing interest in installing grid-connected renewable resources such as wind, solar and tide [1-3]. This trend is attributed to economic and technical benefits of distributed generation DGs in smart grids [4]. On the other hand, DGs require efficient power conditioning converters to adjust their duty cycles to obtain stable MPP under different environmental conditions [1, 2]. It should be noted that wind and solar energy are not only intermittent but also are hardly predictable resources. On the other side, tidal current is intermittent but easily predictable and relies on the same technology of wind turbine. In this respect, the tidal current speed is lower than wind speed, while the water density is higher than air density [2,3].

The energy management of hybrid resources is a complex task. During low solar radiation conditions, photovoltaic (PV) panel cannot ensure the required solar generation. Similarly, wind turbine will not turn until the wind speed is equal to or greater than its cut-in value [2,3]. Therefore, the main objective of power management is to ensure efficient, stable system operation and to prevent energy deficit in grid loads. The real time communication in smart grid can facilitate the generation coordination and then enhance system performance [4].

The technical-environmental studies result in effective replacement of combustion engine-based cars with the electric vehicles (EVs) [5,6]. Through vehicle-to-grid (V2G) technology, the plug-in electric vehicles (PEVs) can be used as energy storage batteries (SB) and can discharge electrical energy back to smart grid. This means that PEVs can support the grid by regulating its voltage and frequency. This support relies on smart grid technology to enable effective utilization of variable renewable resources and electric vehicles [4-6].

The paper is organized as follows: the modeling of different renewable resources are discussed in Section 2. On the other hand, Section 3 extensively reviews the interaction of the EVs with the smart grid. Moreover, in Section 4, a comprehensive case studies are performed using Matlab/Simulink to validate the proposed approach under real metrological date in Kuwait. Finally, the conclusions of the paper are drawn in Section 5.

2. Modeling of Hybrid Renewable Resources

The configuration of proposed hybrid energy system is displayed in Fig. (1). It consists of offshore wind farm, photovoltaic (PV) panels, tidal current turbines, EVs (SB), and electric load.

2.1 Wind Turbine Modeling

Offshore wind energy will be a significant renewable energy source. The range of offshore wind speed

variation is higher than onshore speed. Variable speed turbines using double-fed induction generator (DFIG) are used in recent wind farms [3, 6]. The available wind power P_w in blades swept area (A) is given by:

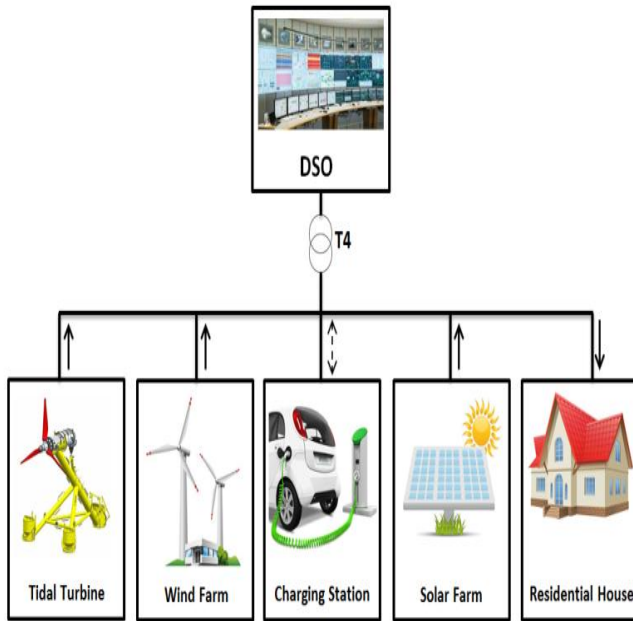


Fig. (1) Hybrid Energy Resources Integration into Electric Grid with EVs

$$P_w = \frac{1}{2} \rho A (V_w)^3 \quad (1)$$

Where, ρ is the density of air and V_w is the wind velocity m/s. The turbine can capture only a fraction of this wind power, which can be expressed as P_m , given by

$$P_m = \frac{1}{2} \rho A (V_w)^3 \cdot C_p(\lambda, \beta) \quad (2)$$

Where, C_p is the captured power coefficient. The maximum theoretical power extracted by an ideal wind turbine is limited to 59.26% of the power available in the wind [7]. The power coefficient $C_p(\lambda, \beta)$ of equation (2) is expressed as a function of tip speed ratio λ and pitch angle β . Any change in the rotor speed and/or wind speed results in a change in tip speed ratio leading to new operating point on the power curves for various speeds and pitch angles [3, 7]. For rated wind speed, the generating power equals the nominal power of the turbine. If the wind speed continues to increase the output power will be theoretically increased until the nominal turbine power. Further wind speed increase can damage the turbine. By turbine over-speed protection, the turbine will shut down if the speed exceeds its maximum permissible value [13].

2.2 Grid connected PV systems

Generally, PV cells are grouped together in similar modules which are interconnected either in series or parallel to form the final PV array. The current-voltage relation of PV array can be mathematically given by [8,9]:

$$I = N_p I_{ph} - N_p I_o \left[\exp^{\frac{qV}{A K T N_s}} - 1 \right] \quad (3)$$

Where,

q : electron charge.

A : P-N junction ideality factor

K : Boltzmann constant.

I : Array output current.

I_{ph} : photocurrent as function of irradiation level and junction temperature

I_o : reverse saturation current of diode.

T : reference cell operating temperature.

V : Array output voltage.

The array output power is determined through multiplying equation (1) by array voltage and efficiency η . Equation (3) indicated that PV array exhibits a non-linear relation of the I-V and P-V characteristics. From P-V curve, there is a specific point at which the generated power is maximum. Therefore, a continuous adjustment of the array terminal voltage is required to extract maximum power (MPP) from the solar array.

The main components of the PV system consist of the solar array, DC/DC smart converter. In this paper, the generated voltage of the PV panel is adjusted to the suitable level corresponding to the maximum solar power using P&O method [1]. In P&O, the operating voltage of the studied PV array is perturbed by a small increment, and the resulting change of power, ΔP is used to update the array voltage as follows:

- If $\Delta P < 0$ & $V(j) > V(j-1)$, then $V(j+1) = V(j) - \Delta V$
- If $\Delta P < 0$ & $V(j) < V(j-1)$, then $V(j+1) = V(j) + \Delta V$
- If $\Delta P > 0$ & $V(j) < V(j-1)$, then $V(j+1) = V(j) - \Delta V$
- If $\Delta P > 0$ & $V(j) > V(j-1)$, then $V(j+1) = V(j) + \Delta V$

2.3 The Tide Energy Model

The total kinetic power in a tidal stream is given by $P_{ts} = \frac{1}{2} \rho A (V_{tide})^3$ [2], where ρ is the water density, V_{tide} is the magnitude of the tide velocity averaged over the cross section A (the turbine area). However, not all this tide power can be converted into mechanical power [3]. This limitation is related to turbine efficiency and is taken into account by the power coefficient (C_p). For tide turbines, the value of C_p ranging between 0.35 and 0.5 [8]. The total mechanical power in a tidal turbine has a similar features as that of a wind turbine [2]. Consequently, the power output may be expressed as:

$$P_t = \frac{1}{2} \rho C_p A (V_{tide})^3 \quad (4)$$

Recently, the selected generator type for the tide energy conversion is the DFIG [8-10]. The objective of the DFIG control is to generate the maximum power under different stream velocities. Therefore, the reference of the rotational speed control loop is adjusted so that the tidal turbine will operate around the maximum power according to the current tidal speed.

3. Integration of EVs into smart grid

The majority of the EV charging systems take place at home. On the other hand, the EV charging is planned to

be undertaken at charging stations in public or working places [4]. However, the integration of the EVs can enhance grid performance, and improve power quality. The modern EVs are developed with a bidirectional grid interface and wireless communication to remotely allow power flow from or to the vehicle. Therefore, an intermediate aggregator has to be developed to coordinate the operation of the grid and vehicles [5]. The aggregator requires the default profiles of all used EVs. These profiles are forwarded by each driver to the aggregator through internet indicating vehicle location, the state of battery charge (SOC) and the availability of V2G implementation. Then corresponding commands are sent wirelessly to the vehicle for exchanging its electrical energy with the grid [4-6].

3.1 Plugged-in Electric Vehicle

The integration of EV can be considered as virtual distributed generation (VDG), where the plugged-in vehicles are clustered and controlled as distributed energy source [11]. Within this VDG concept, the distribution system operator (DSO) has a remote access to the EVs through the aggregator and the stored energy in the vehicle's batteries can participate in the energy supply. The DSO and aggregator are connected over secure communication link. The DSO sends regulation commands to the aggregator to allocate the required regulation capacity from PEVs [6,11]. A schematic diagram of the EV system integration is displayed in Fig.(2). In addition, V2G controller is necessary to control the operation of the plugged-in EVs. In VDG operation, the frequency error will be the input variable to on-line tuned PID controller to balance the generation with load and to regulate the grid frequency. The SOC constraint of EV batteries has to be considered during grid regulation.

The PID controller parameters are on-line tuned by minimizing the integral of time weighted absolute error e in grid frequency (ITAE) given by [12]:

$$ITAE = \int t |e(t)| dt \quad (5)$$

The procedure for on-line parameter tuning using smart grid facilities is summarized in the following steps:

- Initialize the controller parameter
- Simulate the grid behavior and save the time series of the output absolute error $|e(t)|$
- Minimize the ITAE using Matlab optimization function $fminsearch$.
- Update the controller parameters.

3.2 Storage Batteries Model

The surplus of the generated energy by hybrid resources is stored in EV's batteries, and supply this energy back to load during the period of deficit generation taking into account the batteries SOC. The SOC of the battery depends on the previous SOC and the battery energy exchange either in charging or discharging mode during Δt

between two time instants $k, k-1$. In all modes of operation, the SOC is subjected to the following constraint [14, 15].

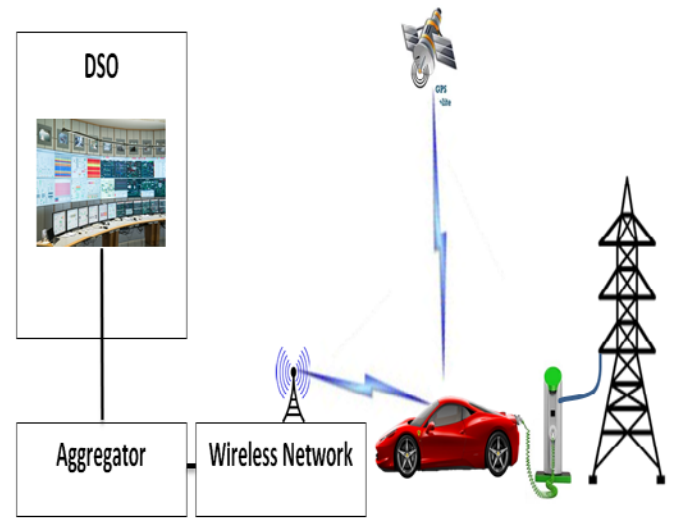


Fig. (2) Configuration of Electric-vehicle to Grid Integration.

$$SOC_{min} \leq SOC_k \leq SOC_{max} \quad (6)$$

Where SOC_k is the state of charge at time instant k , SOC_{min} and SOC_{max} are the minimum and the maximum battery state of charge, respectively. The calculation of SOC depends on the balance between the generated and consumed power at instant k . The hybrid power generation (HPG) at k , can be expressed as follows:

$$HPG_k = P_{pv,k} + P_{w,k} + P_{tid,k} \quad (7)$$

For estimating the SOC_k of EV battery with energy storage capacity (BESC), there are two cases to be considered in expressing SOC_k :

- Case 1: If HPG is greater than load demand (PL) then the SOC_k during charging is given by

$$SOC_k = (SOC_{k-1}) + (HPG_k - PL_k) \Delta t / BESC \quad (8)$$

- Case 2: If PL is equal or greater than the available HPG then the SOC_k during discharging is given by:

$$SOC_k = (SOC_{k-1}) - (HPG_k - PL_k) \Delta t / BESC \quad (9)$$

4. Simulation Results

The knowledge of the weather data are required for appropriate operation of hybrid renewable resources. The statistical analysis of the recorded offshore wind speed shows that the average wind speed for November,

December, January and February are 5.39 m/s, 7.27 m/s, 7.35 m/s and 6.26 m/s respectively. The extreme wind gust speed in the marine area of Kuwait is in the range of 25.5 m/s. In addition, Kuwait has an abundance of solar energy potential. Thereby, the monthly averaged solar intensity on horizontal surface area is 3.26 kWh/m² in December and 8.16 kWh/m² in June. The annual average value of solar radiation reaches 5.9 kWh/m². Moreover, the maximum incident solar radiation matches the peak load in summer.

Generally, tidal currents correlate well with the tidal range and then the tidal current speed can be described by an approximately linear function of the range. For example, on 22th of July of 2017, the sun rose in Kuwait at 5:03 h and sunset was at 18:47 h. The first low tide was at 3:35 h and the next low tide at 17:20 h. The first high tide was at 10:10 h and the next high tide will be at 23:45 h. The recorded height of maximum and minimum tide was 4.1 m and -0.3 m, respectively.

The studied SG consists of 5x900 kW offshore floating wind turbines and 5x1 MW tidal turbines with 22 kV inter-turbine and shore connection submarine cables of Al conductors and embedded optical fibers. The third renewable source is 4 MW PV panels and connected to the grid through smart DC/DC converter and DC/AC, 3-phase two-level inverter. After inversion the arrays are interfaced to the common PCC through 6 kV/22 kV transformer. The whole generation system is connected to the grid at PCC through 20 MVA and 22/132 kV substation.

Due lack of space, the energy supplied by the different renewable resources was calculated for time horizon of 24 hours. The hybrid energy resources of the studied smart grid consists of offshore wind farm, PV array and tidal energy conversion plant with capacity of 4.5, 4 and 5 MW, respectively. These capacities are estimated by generation expansion technique which is outside the scope of this paper. Two types of loads are considered, namely domestic static and small industrial dynamic load of 10 MW and 900 kW, respectively. For this study, the loads and weather data are forwarded to the Simulink model of the smart grid as lookup tables. The simulation of V2G behavior of considered 100 cars with 40 kW each is carried out for the same time scale of 24 hours. The depth of discharge (DOD) of the EV batteries should be equal or greater than 20%.

In this paper, the following three different car-user profiles are considered:

- Possible charge of 40% of EVs from charge station at work.
- No possible charge of 30% of EVs at work
- The rest of EVs with 30% are in charging/ discharging operation mode and can participate in frequency regulation of the grid.

The validity of the developed models is demonstrated using the described models in section 2 to extract the maximum power from different renewable resources. The charging/ discharging characteristics of EVs batteries is

considered to reduce its fluctuations under abnormal conditions and load variations.

Fig. (3) shows the load curve of the studied smart grid. The peak load occurs at 16:00 with a value of 10 MW. The minimum load is at mid-night with 5.8 MW. The maximum and minimum reactive power are 3.3 MVAR and 1.7 MVAR, respectively. To study the behavior of the system under abnormal condition a 3-phase short circuit is simulated at 8:00 for a period of 100 sec. The generated power from PV array can be seen in Fig. (4). As indicated the generated PV power follows the daily variation in the solar radiation and the available solar power has been extracted. The participation of the PV array in supplying the grid load occurs during the period from 6:00 to 17:00. From this figure, it can be observed that the generated power from PV array is decreased to 60 % at 15:00 due to sudden shading for 5 minutes.

In Fig. (5), variation of the power generated by the offshore wind farm is displayed and this power is high when the wind speed is higher than the cut-in speed of 4 m/s. It should be noted that the generated power from the wind farm reaches its maximum value of 4.5 MW for the interval between 21:00 and 22:00, where the wind speed is greater than the rated value of 15 m/s and less than the cut-off speed of 25 m/s. Similarly, Fig. (6) displays the generated power from the tidal plant. The maximum tidal power of 5 MW occurs at 10:00, while the generated power is very small during the period between 16:00 and 19:00 where the tide stream velocity is ranging between 0.48 and 0.74 m/s.

As indicated in the simulation results, the generated power follows the variation of the weather parameters and tracks the maximum power available in the different renewable resources. Furthermore, Fig. (7) shows the daily variation of the state of charge of the plugged-in EV batteries participating in frequency regulation. The SOC starts from a value slightly above 0.9 and decreases during its discharge mode from midnight to 8:00 and charged again during the period of excess renewable generation from 8:00 to 15:00. After that, the SOC is decreased again during night where the PV solar energy is zero and the tidal energy is small.

The charging cycle of the EV profiles is displayed in Fig. (8). The charging intervals and duration depends on the amount of required load and the available renewable generations. Fig. (9) shows the grid frequency obtained by applying V2G concept. The grid frequency at 8:00 deviates from 50Hz (1 pu) due to the short circuit on load bus. The second frequency deviation occurs at 15:00 due to sudden decrease in generated PV power by shading effect. The initial controller parameters K_p, K_i and K_d are 3, 2 and 1, respectively. The final on-line tuned parameters by minimizing ITAE are 1.49, 0.92 and 0.52, respectively. The simulation results indicate that the proposed on-line tuned controller reduces grid frequency fluctuations.

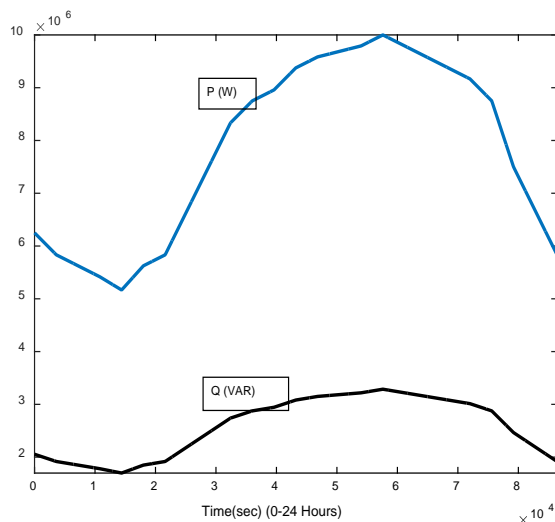


Fig. (3) Active and reactive daily load curve

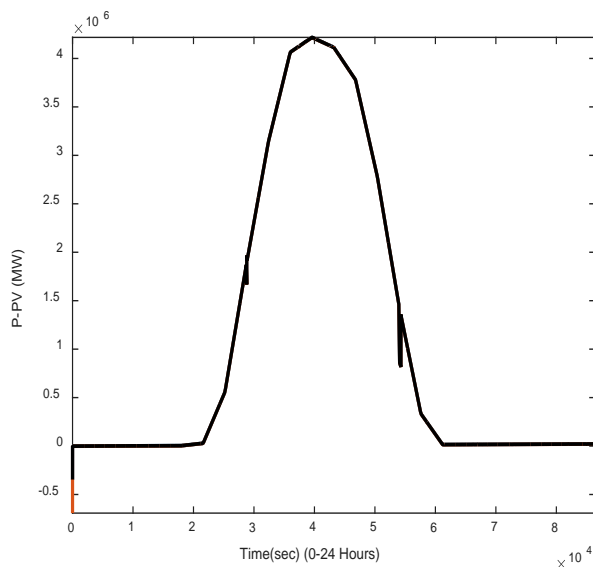


Fig. (4) Generated power from PV array

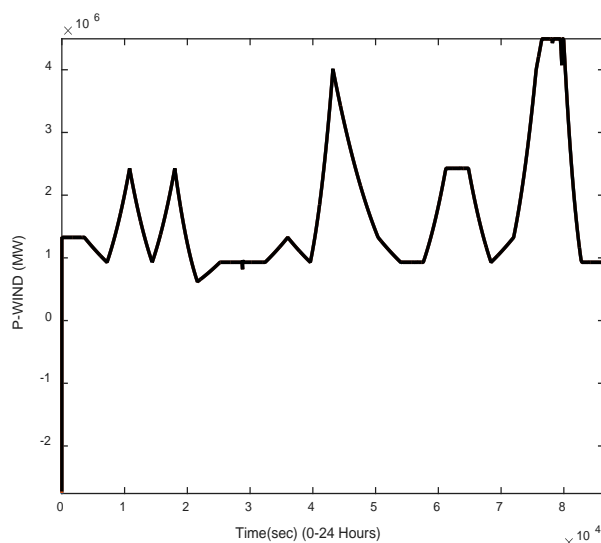


Fig. (5) Generated power from offshore wind farm

5. Conclusions and future research

For efficient utilization of hybrid renewable resources, it is necessary to install smart converters to extract the maximum power of these resources. Matlab/ simulink models have been developed for offshore wind, solar and tide plants. The generated power from these resources was simulated using the actual recorded weather data in Kuwait. The simulation results indicated that the generated energy was tracking the maximum available power of the renewable resources.

In addition, this paper has presented the interaction of electric vehicles with the smart grid containing renewable energy sources. This interaction can provide ancillary services to the grid through frequency regulation by deployment of the described V2G concept. This can be achieved utilizing advanced communication and on-line control strategies of smart grids.

The on-line parameters tuning algorithm of the PID controller has been developed to regulate the grid frequency. This parameter tuning has been achieved by minimizing the integral of time weighted absolute error in grid frequency based on smart grid facilities. The digital simulation of the studied grid has indicated that ITAE tuning method is very effective for eliminating the frequency error and reducing its oscillations during grid disturbances. However, cost-benefit analysis is required to justify future implementation of the V2G in energy market. Moreover, further studies are needed to develop EV batteries with high energy density and extended lifetime under frequent charging and discharging cycles.

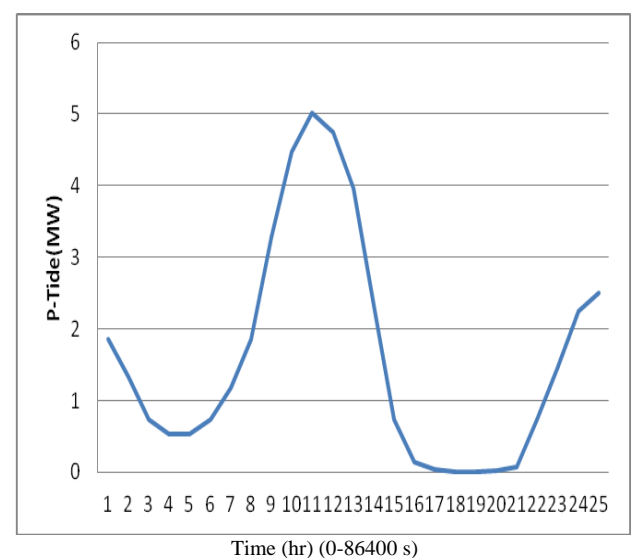


Fig (6) Generated power from tide plant

References

- [1] M. El-Sayed, S. Leeb, "Fuzzy Logic Based Maximum Power Point Tracking Using Boost Converter for Solar Photovoltaic System in Kuwait", *Renewable Energy and Power Quality Journal (RE&PQJ)* ISSN 2172-038X, No. 13, April 2015.
- [2] O. Mohammed, Y. Amirat, M. Benbouzid, S. Haddad, G. Feld, "Optimal sizing and energy management of hybrid wind/tidal/PV power generation system for remote areas: Application to Quessant French Island", *IECON*, Florence, Italy, 24-27 Oct. 2016.
- [3] H. Hamed, H. Aly, M. El-Hawary. "The Current Status of Wind and Tidal in-Stream Electric Energy Resources", *American Journal of Electrical Power and Energy Systems*. Vol. 2, No. 2, 2013, pp. 23-40.
- [4] F. Mwasilu, J. Justo, E.-K. Kim, T. Du, J.-W. Jung, "Electric vehicles and smart grid interaction: A review on vehicle to grid and renewable energy resources integration", *Renewable and sustainable energy review*, 34, pp. 501-516, 2014.
- [5] Darabi Z, Ferdowsi M. "Aggregated impact of plug-in hybrid electric vehicles on electricity demand profile", *IEEE Trans. on Sustain Energy* 2011;2(4):501-8.
- [6] Hugo Morais, Tiago Sousa, Morten Lind, "Electric vehicle fleet management in smart grids: A review of services, optimization and control aspects", *Renewable & Sustainable Energy Reviews*, Vol. 56, 2016, pp. 1207-1226.
- [7] Boukhezzara, B., Lupua, L.; Siguerdidjanea, H., and Hand, M., "Multivariable control strategy for variable speed, variable pitch wind turbines", *Renewable Energy*, vol.32, pp.1273-1287, 2007.
- [8] Weidong Xiao, William G. Dunford, Patrick R. Palmer, Antoine Capel, "Regulation of photovoltaic voltage", *IEEE Trans. on Industrial Electronics*, Vol. 54, No.3, June 2007.
- [9] T. Esram and P. Chapman, "Comparison of Photovoltaic array maximum power point tracking techniques," *IEEE Transactions on Energy Conversion*, Vol. 22, no. 2, Jun. 2007, pp. 439-449.
- [10] S.E. Ben Elghali, M.E.H. Benbouzid and J.F. Charpentier, "Marine tidal current electric power generation technology: State of the art and current status," *Proceedings of IEEE IEMDC'07*, Antalya (Turkey), vol. 2, pp. 1407-1412, May 2007.
- [11] E. Sortomme, M. El-Sharkawi, "Optimal scheduling of vehicle-to-grid energy and ancillary service", *IEEE Trans Smart Grid*, 3(1):351-9, 2012.
- [12] F. Martins, "Tuning PID Controllers Using the ITAE Criterion", *International Journal of Engineering Education*, Vol. 21, No. 3, 2005.
- [13] M. Mahfouz, M. El-Sayed, "Wind Gust Protection Algorithm for Unpitched Control Wind Farm", Accepted for presentation at International Conference on Renewable Energies and Power Quality (ICREPQ'18) Salamanca (Spain), 21th to 23th March, 2018.
- [14] Matthieu Dubarry, Arnaud Devie, Katherine McKenzie, "Durability and reliability of electric vehicle batteries under electric utility grid operations: Bidirectional charging impact analysis", *Journal of Power Sources*, Vol. 358, 1 August 2017, Pages 39-49.
- [15] Kotub Uddin, Tim Jackson, Widanalage D. Widanage, Gael Chouchelamane, Paul A. Jennings, James Marco, "On the possibility of extending the lifetime of lithium-ion batteries through optimal V2G facilitated by an integrated vehicle and smart-grid system" *Energy*, Volume 133, 15 August 2017, Pages 710-722.

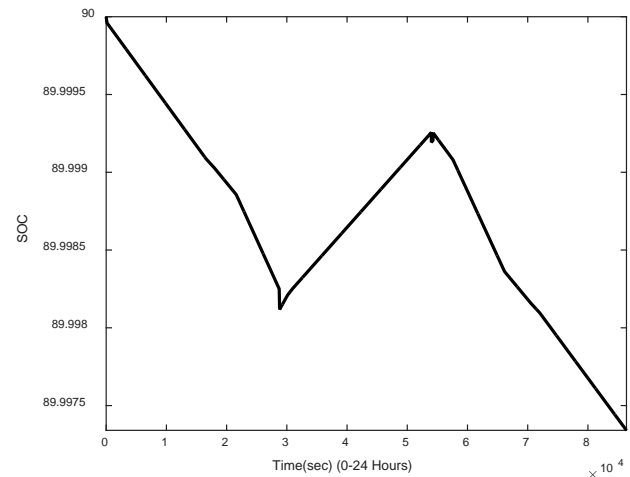


Fig. (7) Variation of Daily state of Charge

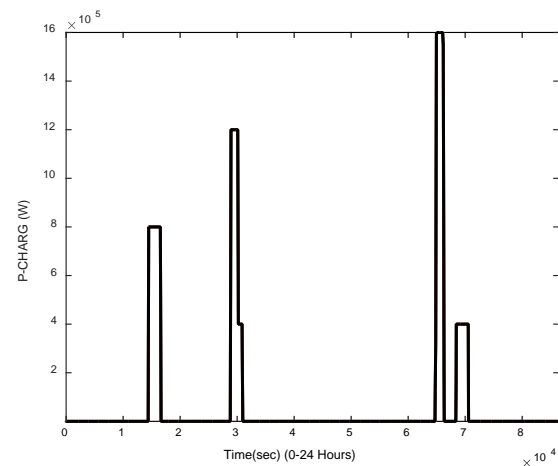


Fig. (8) Charging power of EV-batteries

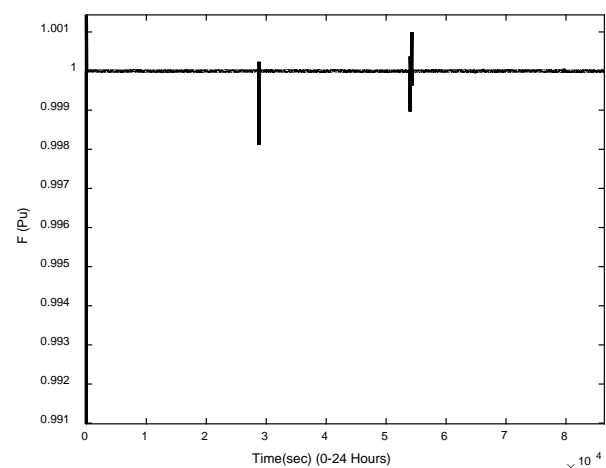


Fig. (9) Frequency variation under load and generation excursion.